OPTICAL PROPERTIES OF PbS-GO AND PbS-rGO SYSTEM FOR SOLAR CELLS FABRICATION

[1]Anton BABAEV, [1]Aliaksei DUBAVIK, [1]Sergei CHEREVKOV, [1]Peter PARFENOV,
[1]Elena USHAKOVA, [1]Mikhail BARANOV, [2]Igor NABIEV,
[1]Alexandr BARANOV, [1]Aleksandr LITVIN

[1]ITMO University, Saint-Petersburg, Russian Federation, a.a.babaev@corp.ifmo.ru
[2]Research Nuclear University MEPhI, Moscow, Russian Federation

Abstract

Quantum dots (QDs) are of great interest for creating optoelectronic devices due to their tunable bandgap, high stability and simple solution processability for device fabrication. One of the ways to increase the efficiency of such devices is to combine QDs with different carbon nanostructures. Lead sulfide PbS QDs with a ligand shell of oleic acid (OA), methylammonium iodide (MAI) and PbI2 were employed to study the process of charge transfer process between QDs and sheets of reduced graphene oxide (rGO) and graphene oxide (GO). QDs have been linked to graphene sheets by the (3-mercaptopropyl) trimethoxysilane in colloidal solution. As a result, we observed a change in intensity and kinetics of QDs PL, that allowed to estimate the efficiency of the charge transfer. The transfer efficiency for the QD-rGO system was found to be higher than that of the QD-GO system, ~ 80 % vs. 66 % respectively. Modification of the QDs surface with MAI and PbI_2 allowed to achieve a charge transfer efficiency of up to 83 % and 89 %, respectively.

Keywords: Colloidal quantum dots, reduced graphene oxide, graphene oxide, PbS

1. INTRODUCTION

Lead sulfide colloidal quantum dots (CQDs) have widely spread as a material for optoelectronic devices including photodetectors [1,2], light-emitting diodes [3,4], and solar cells [5-7] due to their huge bandgap tunability, multiple-exciton generation effect and facile solution-processing. Most common tools to improve the properties of such devices are CQDs surface passivation and optimization of the device structure. For example, outstanding stability was achieved in solution-processed CQDs solar cells even in ambient air conditions through surface passivation [8]. Recent advances in QD solar cells fabrication by device architecture engineering, surface passivation and layers optimization led to reported certified power conversion efficiency (PCE) of 11.6 % [9]. However, a lot of challenges is still to go. One of the main problems for PbS based optoelectronic devices is their rapid degradation under the high relative humidity of ambient air. Recently, it was shown that creating hybrid materials with graphene for active layer fabrication results in the reduction of moisture sensitivity in non PbS based devises [10-14] as well, as in PbS based solar cells [15]. Beside this, combing PbS CQDs with graphene materials is a promising way to fabricate highly effective photodetectors [16,17] and phototransistors [18,19]. In such devices, the charge carriers are generated in the CQDs and after this electrons are transported to the graphene layer according to the energy structure of CQDs-graphene/rGO/GO interface that schematically depicted in **Figure 1** for rGO/PbS case. The charge transfer efficiency of this interface limits the efficiency of this type of devices.

In our study we involved time-resolved PL characterization to evaluate the speed of charge carrier transfer speed in the blend of PbS CQDs and rGO/GO sheets. The PbS CQDs were attached to the rGO and CO sheets using the organic linker molecule. Moreover, the surface of QDs was modified by PbI_2 and MAI to improve the CQDs quality and optimize the charge transfer efficiency.

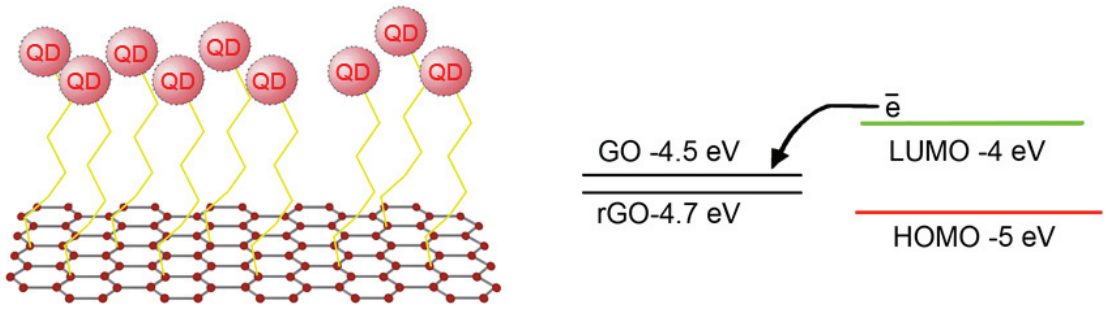

Figure 1 Schematic energy diagram of PbS-rGO

2. MATERIALS AND METHODS

Stabilized with poly(sodium 4-styrenesulfonate) rGO and GO water dispersions were purchased in Sigma-Aldrich (900197 and 777676 aldrich). Moreover, we prepare thin films from both dispersions to ensure the parameters of materials using SEM and AFM. **Figure 2** illustrates a typical single rGO sheet. The thickness we found trough AFM measurements was approximately 1 nm for both materials.

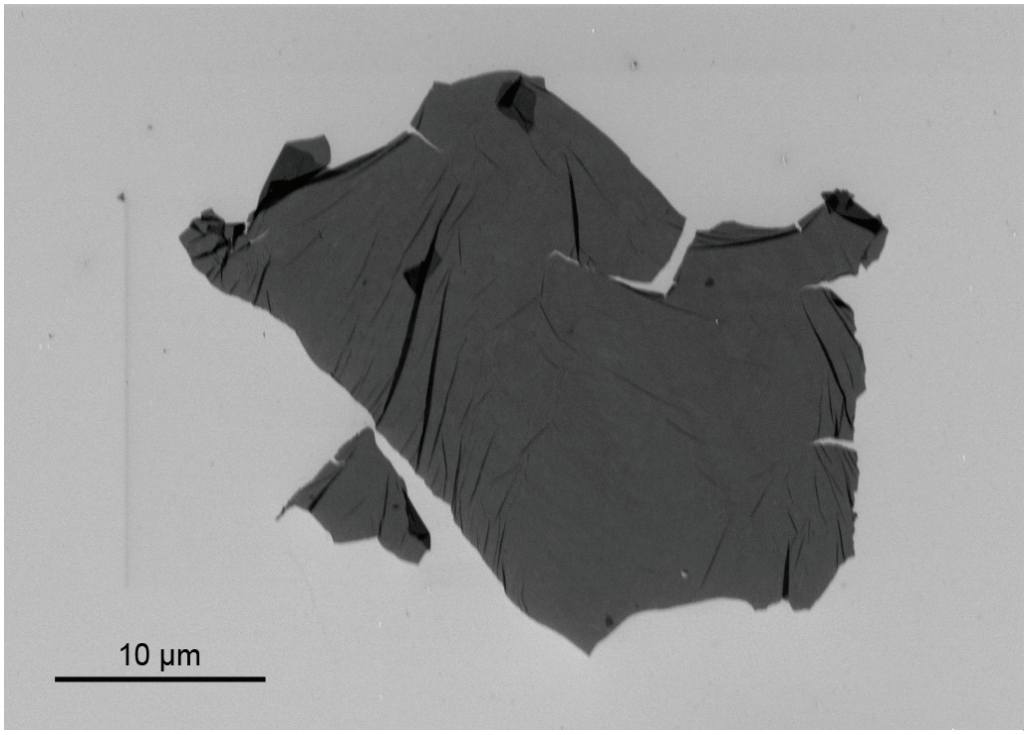

Figure 2 SEM image of rGO sheet

The oleic acid (OA)-capped PbS CQDs were synthesized via well-known protocol from [20]. Briefly, 1 mmol PbO (99.99 %, Aldrich), 4 mmol OA (90 %, Fisher) and 10 ml octadecene (ODE) (90 %, Acros) were mixed in the three-neck 25 ml for Pb precursor preparation. The mixture was heated up to 170 °C under vacuum for approximately 30 minutes until clarification and flushed with Ar. At T=134 °C the mixture of 0.2 mmol hexamethyldisilathiane ($[TMSi]_2S$) in 0.5ml ODE was swiftly injected and heated for 10 min. The reaction was quenched by cooling down in Ar atmosphere and by the addition of acetone to precipitate the PbS nanocrystals. The solution was centrifuged (6000 rpm, 10 min), redispersed in hexane (Sigma-Aldrich) and

precipitated 2 more times with acetone. The final nanocrystals were redissolved in toluene for further use and measurements.

The iodide-capped PbS was obtained by modifying OA-capped PbS via protocol from [21]. In short, 0.02 M PbI_2 solution in 12 ml of dimethylformamide (DMF) and 6 ml of methanol was injected into a suspension of as-prepared PbS nanocrystals (2 mL, 50 mg mL^{-1}). The resulting solution was shaken for 1−2 min, leading to a precipitation of the PbS nanocrystals. After centrifugation, the PbS nanocrystals were redispersed in a mixture of 1,2-dichlorobenzene (DHBZ)(1 mL) and butylamine (BA) (0.2 mL). MAI treatment as well was provided using OA-capped PbS in the prolonged protocol described in [22].

The CQDs were attached with the rGO/GO sheets using 3-mercaptopropyltrimethoxysilane(MPTS), as described in [23]. For MPTS treatment of CQDs, MPTS was added in toluene/DHBZ:BA/DMF OA/iodide/MAI-capped CQDs solution with vortexing for 2 minutes. The solution was precipitated by acetone with centrifugation (6000 rpm, 10 min) and redispersed in the initial solvent.

3. RESULTS AND DISCUSSION

We prepared a series of samples to make our calculations precise. In the beginning, we simply spin-cast GO and OA-capped PbS CQDs layers one after another and observed no decrease in PL lifetime compared to the OA-capped PbS CQDs on the glass. In this case, OA acts like isolator and further, we believe that the change in PL kinetics was induced by the charge transfer process. Otherwise, when the iodide-capped PbS CQDs were spin-coated on GO layer we observe the 30 % decrease of the PL lifetimes because iodide shell is conductive. Then, we mix CQDs by the MPTS. On **Figure 3** one can observe the Pl spectra from OA-capped PbS CQDs in toluene, MPTS-treated OA-capped PbS CQDs in DMF and OA-capped PbS CQDs - MPTS - GO blend in DMF. MPTS treatment results in redshift in spectra accompanied by an increase of PL lifetimes. Such behavior is in contrast to the [23], where 11-mercaptoundecanoic acid treatment was provided to obtain reference PL lifetimes and results in a decrease of PbS CQDs PL lifetimes. We believe the change in surface passivation and medium permittivity affect our CQDs in this way. However, the difference in synthetic protocols and in the applied chemical treatment can explain such discrepancy in the results.

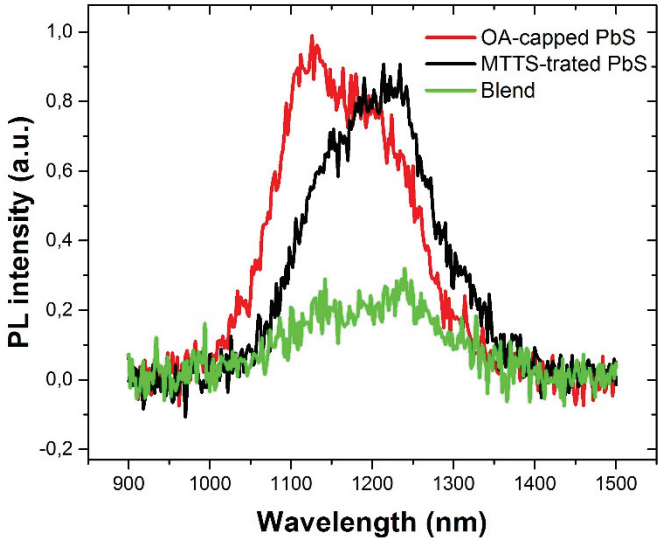

Figure 3 PL spectra of the OA-capped PbS, OA-capped PbS treated with MPTS and OA-capped PbS - GO blend

For all of our blend samples we provide our calculations via the next two equations from [24] and [23]:

$$k_{et} = \frac{1}{\tau_{blend}} - \frac{1}{\tau_{ref}} \quad (1)$$

where:

k_{et} - the rate of electron transfer

τ_{blend} - the decay time of QD-GO/rGO blend

τ_{ref} - the decay time of MPTS treated CQDs

$$\eta = \frac{k_{et}}{k_{et}+k_{rad}+k_{trap}} = 1 - \frac{k_{ref}}{k_{blend}} \quad (2)$$

where:

k_{rad} - the radiative decay rate

k_{trap} - the rate of trapping carriers on CQDs surface

k_{ref} - the decay rate of MPTS treated CQDs

k_{blend} - the decay rate of QD-GO/rGO blend

Our calculations for the samples are given in **Table 1**. This is noticeable that transfer speed calculations give opposite results to the efficiency calculations in the case of OA-capped CQDs and MAI-capped CQDs. In this case the different shell compositions result in different k_{trap} and k_{rad} rates, what counts like ($\Delta k_{trap} + \Delta k_{rad}$) linear mistake for decay rates calculations and like a nonlinear mistake in efficiency calculations. Both parameters for iodide-capped CQDs case are outstanding in comparison to all other structure types. It is obvious that the iodide shell around the CQDs core provides easier charge transfer because of better conductivity.

Table1 The charge transfer rate and efficiency of the charge transfer rate for the obtained samples

Sample	k_{et}, $s^{-1} \cdot 10^6$	η, %
OA capped PbS+rGO	6.8	80
Iodide capped PbS+rGO	7.4	89
MAI capped PbS+rGO	6.6	83
OA capped PbS+GO	4.3	66

Figure 4 illustrates the formation of a spin-coated film from our solution. There are rGO sheets densely occupied by the CQDs. It should be emphasized, that the values of charge transport efficiency strongly depend on the CQDs-rGO proportion. For our study, we employ actual proportions that result in effective device following [6]. The enlargement of rGO content results in the further decay of PL lifetime. For example, 10-time amplification of the rGO content in MAI capped PbS+rGO blend leads to an increment of decay rate to k_{et}=17.9 and transfer efficiency to η=93 %. However, such blend proportions do not result in high performance in despite better charge transfer.

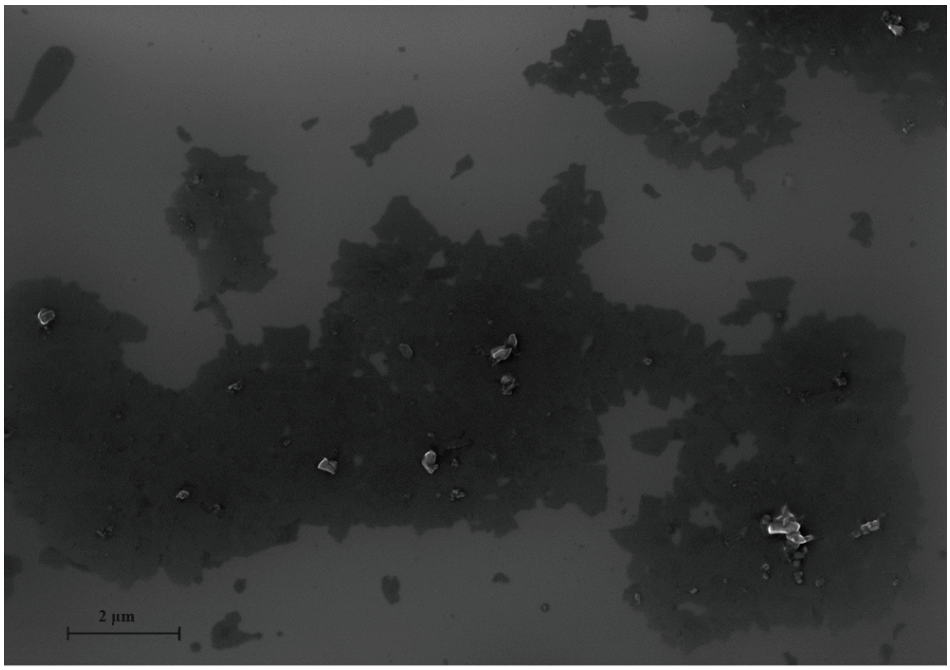

Figure 4 SEM image of the spin-coated film of OA-capper PbS-GO blend

4. CONCLUSIONS

Our group produced a series of experiments that clarify the PbS-rGO/GO charge transfer mechanism. MPTS organic linker forms a well-defined CQDs-rGO/GO system providing both a mechanical connection between system components and better charge transport. The shell also plays an important role in charge process; the iodide shell affords 89 % charge transport efficiency against 80 % in case of basic OA-capped CQDs. The efficiency and transfer rate values were calculated for real device components proportions. The SEM measurements show that CQDs-rGO/GO system forms layers that similar to the rGO/GO layers. The results of our findings reveal details that could important for engineering of solution-processed photovoltaic devices.

ACKNOWLEDGEMENTS

This study was supported by the Ministry of Education and Science of the Russian Federation through the grant No. 14.584.21.0032 (ID RFMEFI58417X0032)

REFERENCES

[1] KUFER, Dominik, NIKITSKIY, Ivan, LASANTA, Tania, NAVICKAITE, Gabriele, KOPPENS, Frank H. L., and KONSTANTATOS, Gerasimos. Hybrid 2D-0D MoS2-PbS quantum dot photodetectors. *Adv. Mater.* 2015. vol. 27, no. 1, pp. 176-180.

[2] SARAN, Rinku and CURRY, Richard J. Lead sulphide nanocrystal photodetector technologies. *Nat. Photonics.* 2016. vol. 10, no. 2, pp. 81-92.

[3] LITVIN, Aleksandr P., MARTYNENKO, Irina V., PURCELL-MILTON, Finn, BARANOV, Alexander V., FEDOROV, Anatoiy V., and GUN'KO, Yurii K. Colloidal quantum dots for optoelectronics. *J. Mater. Chem. A.* 2017. vol. 5, no. 26, pp. 13252-13275.

[4] GONG, Xiwen *et al.* Highly efficient quantum dot near-infrared light-emitting diodes. *Nat. Photonics*. 2016. vol. 10, no. 4, pp. 253-257.

[5] LIU, Mengxia *et al.* Hybrid organic-inorganic inks flatten the energy landscape in colloidal quantum dot solids. *Nat. Mater.* 2017. vol. 16, pp. 258-263.

[6] LU, Kunyuan *et al.* High-Efficiency PbS Quantum-Dot Solar Cells with Greatly Simplified Fabrication Processing via "Solvent-Curing". *Adv. Mater.* 2018. vol. 30, no. 25, pp. 1-9.

[7] CAREY, Graham H., ABDELHADY, Ahmed L., NING, Zhijun, THON, Susanna M., BAKR, Osman M., and SARGENT, Edward H. Colloidal Quantum Dot Solar Cells. *Chem. Rev.* 2015. vol. 115, no. 23, pp. 12732-12763.

[8] CAO, Yiming, STAVRINADIS, Alexandros, LASANTA, Tania, SO, David, and KONSTANTATOS, Gerasimos. The role of surface passivation for efficient and photostable PbS quantum dot solar cells. *Nat. Energy*. 2016. vol. 1, no. 4, p. 16035.

[9] CHOI, Jongmin *et al.* Chloride Passivation of ZnO Electrodes Improves Charge Extraction in Colloidal Quantum Dot Photovoltaics. *Adv. Mater.* 2017. vol. 29, no. 33, p. 1702350.

[10] LIU, Zhike, LAU, Shu Ping, and YAN, Feng. Functionalized graphene and other two-dimensional materials for photovoltaic devices: device design and processing. *Chem. Soc. Rev.* 2015. vol. 44, no. 15, pp. 5638-5679.

[11] GUO, Yunlong, LIU, Chao, TANAKA, Hideyuki, and NAKAMURA, Eiichi. Air-Stable and Solution-Processable Perovskite Photodetectors for Solar-Blind UV and Visible Light. *J. Phys. Chem. Lett.* 2015. vol. 6, no. 3, pp. 535-539.

[12] LEE, Seungae, KIM, Yun Ki, and JANG, Jyongsik. Long-term stability improvement of light-emitting diode using highly transparent graphene oxide paste . 2016. vol. 8, p. 17551.

[13] GLEN, Tom S. *et al.* Dependence on material choice of degradation of organic solar cells following exposure to humid air. *J. Polym. Sci. Part B Polym. Phys.* 2016. vol. 54, no. 2, pp. 216-224.

[14] BAI, Yang *et al.* Enhancing stability and efficiency of perovskite solar cells with crosslinkable silane-functionalized and doped fullerene, *Nat. Commun.* 2016. vol. 7, p. 12806.

[15] MARTÍN-GARCÍA, Beatriz *et al.* Reduction of moisture sensitivity of PbS quantum dot solar cells by incorporation of reduced graphene oxide. *Sol. Energy Mater. Sol. Cells*. 2018. vol. 183, no. March, pp. 1-7.

[16] NIAN, Qiong, GAO, Liang, HU, Yaowu, DENG, Biwei, TANG, Jiang, and CHENG, Gary J. Graphene/PbS-Quantum Dots/Graphene Sandwich Structures Enabled by Laser Shock Imprinting for High Performance Photodetectors. *ACS Appl. Mater. Interfaces*. 2017. vol. 9, no. 51, pp. 44715-44723.

[17] GONG, Maogang *et al.* Printable Nanocomposite FeS_2 -PbS Nanocrystals/Graphene Heterojunction Photodetectors for Broadband Photodetection. *ACS Appl. Mater. Interfaces*. 2017. vol. 9, no. 33, pp. 27801-27808.

[18] SONG, Xiaoxian *et al.* Graphene and PbS quantum dot hybrid vertical phototransistor, *Nanotechnology*. 2017. vol. 28, no. 14, p. 145201.

[19] CHE, Yongli *et al.* High-performance PbS quantum dot vertical field-effect phototransistor using graphene as a transparent electrode. *Appl. Phys. Lett.* 2016. vol. 109, no. 26, p. 263101.

[20] USHAKOVA, Elena V. *et al.* Anomalous size-dependent decay of low-energy luminescence from PbS quantum dots in colloidal solution. *ACS Nano*. 2012. vol. 6, no. 10, pp. 8913-8921.

[21] LU, Haipeng, JOY, Jimmy, GASPAR, Rachel L., BRADFORTH, Stephen E., and BRUTCHEY, Richard L. Iodide-Passivated Colloidal PbS Nanocrystals Leading to Highly Efficient Polymer:Nanocrystal Hybrid Solar Cells. *Chem. Mater.* 2016. vol. 28, no. 6, pp. 1897-1906.

[22] LAN, Xinzheng *et al.* 10.6 % Certified Colloidal Quantum Dot Solar Cells Via Solvent-Polarity-Engineered Halide Passivation. *Nano Lett.* 2016. vol. 16, no. 7, pp. 4630-4634.

[23] MARTÍ N-GARCÍ, Beatriz, POLOVITSYN, Anatolii, PRATO, Mirko, and MOREELS, Iwan. Efficient charge transfer in solution-processed PbS quantum dot-reduced graphene oxide hybrid materials. *J. Mater. Chem. C*. 2015. vol. 7088, p. 7088.

[24] JARZAB, Dorota, SZENDREI, Krisztina, YAREMA, Maksym, PICHLER, Stefan, HEISS, Wolfgang, and LOI, Maria A. Charge-separation dynamics in inorganic-organic ternary blends for efficient infrared photodiodes. *Adv. Funct. Mater.* 2011. vol. 21, no. 11, pp. 1988-1992.